MAGNETIC RESONANCE IN CHEMISTRY
Magn. Reson. Chem. 2000; **38**: 596–603

Solid-state NMR study of the SH3 domain of α-spectrin: application of $^{13}C-^{15}N$ TEDOR and REDOR†

Sven Macholl,[1] Ingolf Sack,[1]‡ Hans-Heinrich Limbach,[1] Jutta Pauli,[2] Mark Kelly[2] and Gerd Buntkowsky[1]*

[1] Institut für Chemie, FU Berlin, Takustr. 3, D-14195 Berlin, Germany
[2] Abteilung NMR-unterstützte Strukturforschung, FMP Berlin, Alfred-Kowalke-Str. 4, D-10315 Berlin, Germany

Received 28 January 2000; revised 11 March 2000; accepted 11 March 2000

ABSTRACT: A fully $^{13}C-^{15}N$-labeled and a selectively alanine-$^{13}C^{\beta}$ tryptophan-$^{15}N^{ring}$-labeled sample of the Src homology region 3 (SH3) domain of α-spectrin (chicken), a 62 residue protein, were biosynthesized and studied by solid-state cross-polarization magic angle spinning (CP/MAS) NMR, $^{13}C-^{15}N$ rotational echo double resonance (REDOR) and $^{15}N-^{13}C$ transferred echo double resonance (TEDOR) spectroscopy. In the first part of the study it is shown that spectral editing with the TEDOR sequence leads to a drastic simplification of the ^{13}C MAS spectrum of the fully labeled sample, allowing the resolved spectroscopy of groups of ^{13}C nuclei, according to their distance to neighboring ^{15}N nuclei. In the second part of the study the inter-residual distance between the alanine residue Ala55 and the tryptophan residue Trp42 was determined by the measurement of the dipolar coupling between Ala-$^{13}C^{\beta}$ and Trp-$^{15}N^{ring}$, yielding a dipolar coupling of 48 ± 8 Hz, which after correction for fast molecular vibrations gives a value of 53 ± 8 Hz, corresponding to a CN distance of 3.85 ± 0.25 Hz. The result is compared to the CN distances obtained by x-ray diffraction and liquid-state NMR. Copyright © 2000 John Wiley & Sons, Ltd.

KEYWORDS: SH3 domain; α-spectrin; protein; TEDOR; REDOR; spectral editing; chemical editing; CN distances; dipolar solid-state NMR

INTRODUCTION

The biological function of a protein is mainly determined by two factors, the primary structure, i.e. its amino acid sequence, and the geometrical arrangement of the amino acid chain and the side groups, i.e. its secondary and higher structures.[1] The primary structure of peptides and proteins of interest is known in general or can be determined by standard techniques. The determination of the higher structures is more elaborate. If suitably crystallized samples of the protein are available, it is possible to determine these higher structures by x-ray diffraction. An alternative approach is multi-dimensional liquid-state NMR spectroscopy of dissolved molecules.[2,3] Both of these methods have their limitations: on the one hand, many proteins are not available in single-crystal form, for example owing to poorly crystallizing behavior. On the other hand, proteins often exceed the range of molecular weights suitable for liquid-state NMR studies, are only poorly soluble or tend to aggregate. Furthermore, the important group of membrane embedded proteins cannot be analyzed by x-ray diffraction or solution NMR.

Solid-state NMR spectroscopy[4,5] can help in structural studies of these classes of proteins. Because of the special experimental requirements of this type of NMR, this approach is still under development. Two major problems have to be solved before a successful solid-state structural analysis of a protein is feasible. First, the spectral resolution has to be increased to achieve a resolution comparable to the resolution in liquid-state NMR. Second, techniques for monitoring neighbor relationships of different amino acid residues have to be developed, applied and combined with efficient techniques for distinguishing between the contributions from different types of interactions.

One approach for the study of proteins with solid-state NMR relies on orienting the sample with respect to the magnetic field B_0, e.g. by embedding the protein in a membrane. Orientation constraints are derived from dipolar couplings and chemical shift interactions, the values of which depend on the relative alignment of the molecule with respect to the external field.[6,7] This technique is restricted to a limited class of proteins. Therefore, magic angle spinning (MAS)[8,9] NMR techniques and in particular the cross-polarization (CP) MAS experiment[10,11] have provided the major means to solve the resolution problem. The linewidths typically obtainable by MAS are in most cases still an order of magnitude worse than those typically found in liquid-state NMR. Only very recently with the development of high-speed ^{13}C CP/MAS probes and high-field solid-state NMR spectrometers do linewidths suitable for real high resolution in the solid state seem to be achievable.

† This paper is dedicated to Professor Dr Harald Günther on the occasion of his 65th birthday.

* *Correspondence to*: G. Buntkowsky, Institut für Chemie, FU Berlin, Takustr. 3, D-14195 Berlin, Germany; e-mail: bunt@chemie.fu-berlin.de
‡ Present address: Department of Chemical Physics, The Weizmann Institute of Science, Rehovot 76100, Israel.
Contract/grant sponsor: German Israel Foundation; *Contract/grant number*: GIF I-595-43.09/98.

Two prerequisites are needed for a successful structure determination by MAS NMR spectroscopy: (i) a high spectral resolution to assign individual lines to particular atomic positions in the molecule by virtue of their isotropic chemical shift and (ii) a network of adjacency and distance information, which can be found by recording the couplings between different atoms in the molecule.

For the analysis of the distance information under high-resolution MAS conditions, several advanced NMR techniques are now available. A review of some of these techniques was given by Bennett *et al.*[12] and the application of these techniques to biological samples was reviewed by Auger.[13] The basic idea of these techniques is to reintroduce the dipolar coupling in the course of the MAS experiment by periodically disturbing the evolution of the spin system with the r.f. pulses, leading to a dipolar recoupling. For heteronuclear systems of two X-nuclei, the rotational echo double resonance (REDOR) experiment[14–18] is of particular importance. This method allows the recoupling of dipolar interactions between different X-nuclei (e.g. ^{15}N and ^{13}C) by periodically inverting the sign of the dipolar interaction in the course of the experiment. The strength of the dipolar interaction can be determined by performing an echo experiment and measuring the signal decay caused by dipolar dephasing. This decay can be adjusted to a known master curve to determine the strength of the interaction or alternatively it can be transformed into the frequency domain. Examples of some recent applications of dipolar recoupling techniques to proteins and other biomolecules can be found in the literature.[19–29]

The differences in the dipolar dephasing times in the ^{13}C–^{15}N REDOR experiment can be exploited as dipolar filters, which reduce the number of overlapping side-chain signals.[30–33] However, the price for the simplification of the ^{13}C spectrum is a considerable decrease in intensity. Moreover, these editing techniques remove the signal of the dephased nuclei and they cannot be used as building blocks of heteronuclear correlation experiments. For such tasks, active magnetization transfer experiments or coherence transfer techniques are more attractive. In the solid state the active transfer of magnetization from one type of spin-1/2 nuclei to another type of spin-1/2 nuclei, e.g. from ^{15}N to ^{13}C, can be achieved via heteronuclear dipolar couplings.[19,34–39] The TEDOR (transferred echo double resonance[39]) technique is the solid-state NMR analog of the INEPT experiment in liquid-state NMR. After initial cross-polarization of the nucleus I, the evolution of the magnetization under the influence of the heteronuclear dipolar interaction during the time τ_1 creates IS spin coherence, which is converted into S spin coherence by a simultaneous 90° pulse in both I and S channels and a second evolution for the time τ_2. The transfer efficiency is at a maximum if the two delays are equal, i.e. $\tau_1 = \tau_2$. In single crystals or liquids, complete coherence transfer can be achieved by such a technique if the transfer time is chosen correctly. In non-oriented powder samples, however, only a partial transfer is possible, owing to the orientation dependence of the dipolar interactions.

The aim of this work was the evaluation of some solid-state NMR strategies for structural studies of proteins, employing a small protein with known structure as a 'real world' model of large solid proteins. In the first part a strategy for simplification of complex solid-state NMR spectra of fully ^{13}C- and ^{15}N-labeled samples with the help of the TEDOR sequence was assessed. The second strategy combined special chemical editing of the sample with dipolar solid-state NMR spectroscopy. In general, selective chemical editing of a protein sample is not an easy task. In our case we employed a relatively simple chemical labeling scheme by adding a single, selectively ^{13}C-labeled amino acid to the medium for the biosynthesis. With this scheme a selective enrichment of this amino acid in the protein is achieved. This partial enrichment allows even on a non-high-field solid-state NMR spectrometer a faithful determination of non-trivial interresidual distances in a protein.

We choose the chicken (*Gallus gallus*) Src homology region 3 (SH3) domain (Fig. 1) of α-spectrin as a model system for our studies for several reasons. (i) With its 62 amino acids it is a relatively small protein including a great variety of 18 different amino acids. This results in a relatively wide distribution of ^{13}C chemical shifts in the NMR spectrum and therefore a minimum signal overlap, which allows for a reasonable resolution even on a non-high-field solid-state NMR spectrometer. (ii) The samples used in the presented NMR experiments are stable against heat-induced molecular conformation changes. The solid-state ^{13}C and ^{15}N NMR spectra both displayed constant chemical shifts over a period of several months indicating a high structural stability of the SH3 domain. (iii) The structure of the SH3 domain has been analyzed by x-ray diffraction with a resolution of 1.8 Å. This allows control of the structural data obtained by solid-state NMR.

The first reported crystal structure of an SH3 domain is that of the α-spectrin SH3 domain (chicken).[40] Spectrin is the major component of the cytoskeleton that underlies the cell membrane. It has an SH3 domain inserted into one structural repeat of the α-chain. This SH3 domain is a good model system for protein folding and stability

Figure 1. X-ray structure of the backbone of the SH3 domain and the positions of tryptophan residue Trp42 and alanine residue Ala55. The arrow marks the distance from the $^{13}C^{\beta}$ (Ala55) to the $^{15}N^{ring}$ (Trp42). The ^{13}C–^{15}N distance of the $^{13}C^{\beta}$ (Ala55) and the $^{15}N^{ring}$ (Trp42) determined by x-ray diffraction and liquid-state NMR varies in the range 3.56–3.73 Å. Note the relatively large 'free' volume in the vicinity of the Trp42 residue.

studies and in particular for all β-structures of proteins. Its tertiary structure is that of a small scaffold composed of five antiparallel β-strands. The structure has been analyzed again by x-ray diffraction[41] and also by liquid-state NMR spectroscopy.[42] Structures of several other SH3 domains have also been determined. In all these studies, a similar common β-barrel motif was found in spite of the low degree of sequence similarity within the family.[43] The function of the SH3 domain is still not clear, but the proteins, in which the SH3 domain can be found, are often involved in signal transduction pathways (see Musacchio *et al.*[43] and references cited therein).

In principle, it is possible to study directly fully isotope-enriched SH3 protein samples by solid-state NMR. In practice, however, the strong signal overlap will prevent a sufficient resolution of the individual resonances, in particular with a 7 T spectrometer as used in this study. Therefore, the application of spectral or chemical editing techniques is necessary for enhancing the resolution in the NMR experiment.

Both of these techniques have their unique merits and drawbacks. Solid-state NMR spectral editing techniques are very expensive in the sense of signal losses for the following reasons: on the one hand, the T_2 relaxation times of coherences, which are involved in the TEDOR transfer, can be relatively short in the solid state, compared with liquid-state NMR, resulting in a shorter time window for the transfer. On the other hand, the orientation distribution of dipolar coupling in non-oriented powder samples prevents a simultaneous 'resonance' condition for all crystallites in the sample in the course of the TEDOR experiment, as compared with the equivalent INEPT sequence, where the 'resonance condition' is fulfilled for a transfer time of $\tau = 1/(2J)$.

On the other hand, chemical editing of a protein by selectively replacing only some amino acids can be difficult to achieve because of metabolic side reactions which may introduce additional isotope labels in unwanted molecular positions, because the microorganism employed for the biosynthesis digests part of the labeled amino acids and uses the labeled fragments for the biosynthesis of other amino acids.

Both editing techniques were employed in this study: in the first part, the heteronuclear ^{13}C ^{15}N dipolar interaction was employed for spectral editing and thus for simplification of the ^{13}C NMR spectrum of the SH3 domain. In the second part, chemical editing of the SH3 domain was employed and an inter-residual distance between two nuclei of different β-strands was measured. From the known crystal structure of the SH3 domain, it is evident that the residue pair Ala55–Trp42 is a good candidate for such an experiment (Fig. 2).

The rest of this paper is organized as follows: the experimental part consists of an introduction into the REDOR technique for the measurement of heteronuclear dipolar couplings in the solid state, followed by a short overview of the sample preparation and a description of our experimental set-up. Then the experimental results are presented, discussed and finally summarized.

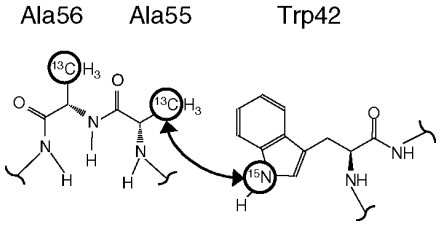

Figure 2. Part of the SH3 domain amino acid sequence displaying the selectively $^{13}C^{\beta}$-labeled alanine residues Ala55 and Ala56 and the $^{15}N^{ring}$-labeled tryptophan residue Trp42.

EXPERIMENTAL

The REDOR experiment

The basic theory of the REDOR experiment[12,14,15] is well known from the literature and will be only briefly summarized here. For a heteronuclear spin-1/2 pair, the solid-state NMR high-field MAS Hamiltonian is given as (J-coupling can be neglected)

$$\hat{H}(t) = \omega_D(t) 2\hat{I}_z\hat{S}_z + \omega_S(t)\hat{S}_z + \omega_I(t)\hat{I}_z \qquad (1)$$

where $\omega_S(t)$ and $\omega_I(t)$ characterize the chemical shift values of the S and I spins, respectively, and $\omega_D(t)$ describes the dipolar coupling between S and I spins. In solid samples, all three frequencies in Eqn (1) are functions of the orientation of the molecule with respect to the external magnetic field, giving rise for non-oriented samples to the well known NMR powder pattern, i.e. broad lines caused by the distribution of resonance frequencies. These broad spectra can be transferred into narrow 'liquid-like' spectra by fast sample spinning around an axis inclined at an angle of 54.7° with respect to the direction of the magnetic field, the so-called magic angle. This sample spinning removes the distance information present in the dipolar part of the Hamiltonian by averaging the dipolar interaction to zero. This information is recovered by the REDOR sequence, an irradiation of two π-pulses during one rotor period T_r, the first at time τ and the second at the end of the rotor period.

The recoupled dipolar frequency of a specific spin packet depends on the orientation of the dipolar vector with respect to the external field, defined by the polar angles α and β

$$\overline{\omega}_D(\alpha, \beta, \tau) = \frac{1}{T_r}\left[\int_0^{\tau} \omega_D(\alpha, \beta, t')dt' - \int_{\tau}^{T_r} \omega_D(\alpha, \beta, t')dt'\right] \qquad (2)$$

with

$$\omega_D(\alpha, \beta, t) = \pm\tfrac{1}{2}D[\sin^2\beta\cos 2(\alpha + \omega_r t) - \sqrt{2}\sin 2\beta\cos(\alpha + \omega_r t)] \qquad (3)$$

The heteronuclear dipolar coupling D, which depends on the distance r of the two nuclei I and S as

$$D = \frac{\mu_0}{4\pi}\hbar\frac{\gamma^I\gamma^S}{r^3} \qquad (4)$$

contains the structural information.

The measured REDOR signal S_R can be expressed as a function of the number N of applied REDOR cycles and the spinning frequency $1/T_r$:

$$S_R(\alpha, \beta) = T_r[\rho(\alpha, \beta)S_x] = \cos\{\overline{\omega}_D(\alpha, \beta, T_r/2)NT_r\} \quad (5)$$

For non-oriented powder samples the integral over the polar angles α and β has to be calculated, yielding the REDOR signal:

$$S_R = \frac{1}{4\pi}\int_{\alpha,\beta} S_R(\alpha, \beta)\sin\beta \mathrm{d}\beta\mathrm{d}\alpha \quad (6)$$

The most efficient dipolar recoupling is achieved if the first π-pulse is irradiated at the center of the rotor cycle, i.e. $\tau = T_r/2$. In this case[44,45] there exists an analytical expression for the REDOR signal [$J_\nu(x)$, cylindrical Bessel function of the first kind; n, number of rotor cycles]:

$$S_R(n\nu_D T_R) = \frac{\pi}{2\sqrt{2}} J_{1/4}(n\sqrt{2}\nu_D T_R)J_{-1/4}(n\sqrt{2}\nu_D T_R) \quad (7)$$

and a direct transformation of the decay function from the time domain into the frequency domain, the so-called REDOR transform.

To take relaxation processes during the REDOR evolution periods (nT_r) into account, a reference experiment under the same conditions but without recoupling pulses is performed. With the reference signal S_0 the normalized dipolar dephasing is given as

$$\frac{\Delta S}{S_0} = \frac{S_0 - S_R}{S_0} \quad (8)$$

Sample preparation

Two different types of isotope-labeled samples were employed, namely a fully $^{13}C-^{15}N$-labeled SH3 sample and a sample which was selectively ^{13}C and ^{15}N labeled: ^{13}C was introduced in the β-position of the three alanine residues present in the SH3 domain (Ala11, Ala55, Ala56) and ^{15}N in the ring of the two tryptophan residues (Trp41, Trp42) and in the side-chains of the two glutamine (Gln16, Gln50) and three asparagine residues (Asn35, Asn38, Asn47).

The fully labeled SH3 domain was prepared in the following way: a plasmid was employed as expression vector for the SH3 domain in the bacterium *Escherichia coli*. The bacteria were grown on nominally 100% $^{15}NH_4Cl$ and nominally 100% ^{13}C-labeled glucose. The aqueous protein solution was dried directly by lyophilization.[25,46] The preparation of the selectively labeled SH3 sample is described in full detail elsewhere.[52] Because of metabolic side reactions in the course of the biosynthesis of the sample, part of the ^{13}C and ^{15}N went to other molecular positions (e.g. ^{15}N into the backbone), resulting in a lower labeling of the target positions. From control measurements with liquid-state NMR, the following labeling factors were estimated: C^β (Ala55), 80% ^{13}C enriched; N^{ring} (Trp42), 65% ^{15}N enriched. No ^{15}N enrichment of the ^{13}C-labeled alanine residues was found. The SH3 precipitated after changing the pH of the SH3 solution from 3.5 to 7.5. The dry mass of the precipitated sample was 12 mg.

The best ^{13}C NMR linewidth of the selectively labeled SH3 domain was obtained by moistening the samples with doubly distilled water.[47] This mushy sample gave a well resolved spectrum of the alanine C^β lines even on our 7 T spectrometer.

The spectrometer

A detailed discussion of our laboratory-built three-channel solid-state NMR spectrometer (wide-bore 6.98 T magnet) has been given recently.[48] All MAS experiments were performed employing a 7 mm Bruker H-XY triple resonance probe. In the triple resonance experiments the typical 90° pulse length was 6.5 µs for all three channels, corresponding to 38 kHz B_1 field in frequency units. For ^1H decoupling, B_1 was changed to 52 kHz to avoid unwanted cross-polarization by mismatching the Hartmann–Hahn condition and to improve the decoupling efficiency. For achieving the optimum decoupling efficiency, the TPPM sequence[49,50] was employed. This in conjunction with MAS was sufficient to remove ^1H-X dipolar line broadening. The rotation frequency (normally 5 kHz) was actively controlled using a Doty spin rate controller. Deviations in the rotation frequency were typically below 2 Hz.

RESULTS AND DISCUSSION

MAS NMR on the fully $^{13}C-^{15}N$-labeled SH3 domain

In a first step, the conventional ^{13}C (Fig. 3) and ^{15}N (not shown) MAS and CP/MAS NMR spectra of the SH3 domain sample were recorded. The ^{13}C spectrum of the SH3 domain exhibits severe line overlap due to the numerous nuclei with similar chemical shifts. The spectrum covers the typical chemical shift range of approximately 250 ppm with four distinct regions: (i) signals of the amide and carboxyl carbons in the range 170–175 ppm; (ii) signals of mainly the backbone α-carbons in the range

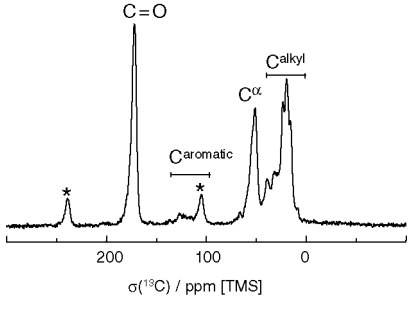

Figure 3. ^{13}C MAS spectrum of the SH3 domain (fully ^{13}C labeled). The asterisks mark the spinning sidebands of the amide carbons.

48–65 ppm; (iii) signals of alkyl carbons in the side-chains in the range 15–25 ppm; and (iv) signals from aromatic side-chain carbons mainly in the range 110–130 ppm.

TEDOR experiments on the fully ^{13}C–^{15}N-labeled SH3 domain

The TEDOR experiment allows spectral editing of a complex spectrum. As an experimental example of such an application of the TEDOR technique, Fig. 4 compares the TEDOR edited ^{13}C spectra of the fully ^{13}C–^{15}N-labeled SH3 domain sample for two different TEDOR transfer times (10 000 scans) to the normal CP/MAS spectrum (2060 scans). It is evident that, despite the five times higher number of scans, the signal-to-noise (S/N) ratio of the TEDOR spectra is much lower than the S/N ratio of the CP/MAS spectrum. The normalized S/N ratio can be estimated as 1 : 0.1 : 0.05. In the reference spectrum, lines of all ^{13}C atoms are visible. The transfer times in the TEDOR experiment were chosen in such a way that only the couplings to one-bond and two-bond neighbors are strong enough to create substantial ^{13}C signals. The TEDOR spectrum obtained after two rotor cycles (400 μs) displays only lines of the backbone α- and amide carbons. After four rotor cycles (800 μs) the side-chain β-carbons also become visible. These results show that such TEDOR techniques can be relatively easily applied to other ^{15}N-labeled systems, where ^{13}C positions at one or two bond distances are to be filtered from the background of ^{13}C positions further away from the ^{15}N. Moreover, it should be noted that the relaxation of the coherences in the TEDOR transfer is probably shortened by homonuclear couplings among the ^{13}C spins. Therefore, one can expect that in diluted ^{13}C systems also larger distances from the ^{15}N label to the ^{13}C nucleus can be filtered with reasonable S/N ratio.

Heteronuclear correlation techniques such as TEDOR can also be employed as building blocks of 2D or more generally multi-dimensional NMR experiments. As an example, Fig. 5 displays a two-dimensional ^{15}N–^{13}C HETCOR via the TEDOR experiment. The pulse sequence starts with CP to the ^{15}N, then an evolution time τ_1 is inserted, followed by the TEDOR transfer to the ^{13}C and detection of the signal in the ^{13}C τ_2 period. The TEDOR transfer time was set to four rotor cycles. The 2D Fourier transformation produces

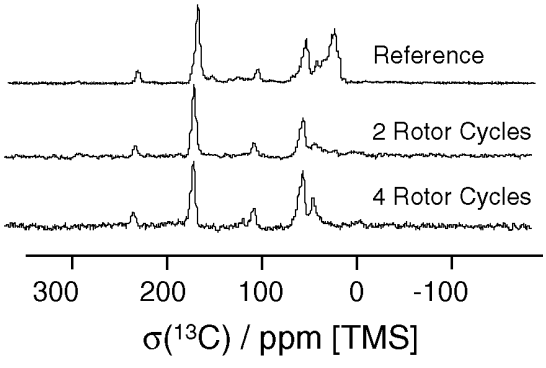

Figure 4. Spectral editing with the TEDOR sequence ($\nu_{rot} = 5$ kHz). The ^{13}C (observed) ^{15}N spectra for $n = 2$ and 4 are compared with the unedited ^{13}C CPMAS spectrum.

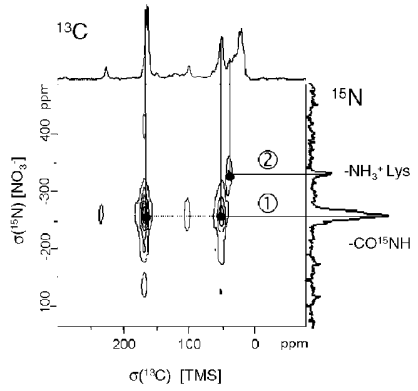

Figure 5. 2D heteronuclear correlation with the TEDOR sequence ($\nu_{rot} = 5$ kHz). First the thermal ^{13}C magnetization is destroyed by a saturation sequence, then the ^{15}N coherence is transferred to the neighboring ^{13}C. The lines mark which carbons are polarized from backbone nitrogen and lysine side-chain nitrogen, respectively.

a resolved MAS spectrum for the two interacting sets of heteronuclei. In the resulting 2D spectrum two types of carbons can be clearly distinguished, namely those which are coupled to backbone ^{15}N and those which are coupled to lysine side-chain ^{15}N nuclei.

MAS and REDOR experiments on the selectively ^{13}C–^{15}N-labeled SH3 domain

This section presents the ^{13}C ^{15}N REDOR results obtained on the selectively labeled SH3 domain sample. In a first step, the MAS spectra of the labeled sample were recorded. Figure 6 displays the ^{13}C MAS spectrum of the sample. The three alanine methyl ^{13}C ($^{13}C^{\beta}$) lines of the residues Ala11, Ala55 and Ala56 are clearly resolved. The unique assignment of the high-field line to the Ala55 residue was possible owing to the observed ^{13}C ^{15}N REDOR effect with the nearby tryptophan ring ^{15}N (see below). The ^{15}N MAS spectrum of the selectively labeled

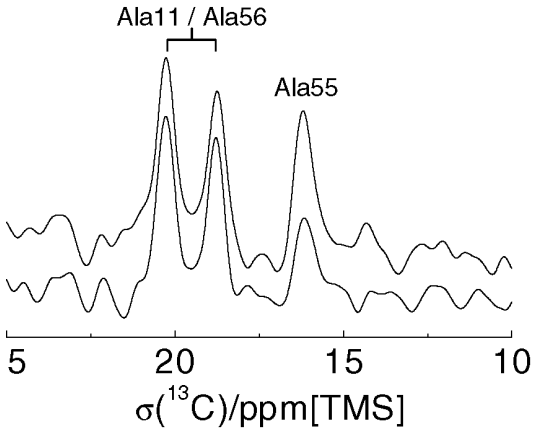

Figure 6. Methyl region of the ^{13}C spectrum of the alanine-$^{13}CH_3$ enriched SH3 domain sample. Upper curve: normal CP/MAS spectrum. Lower curve: REDOR spectrum after a 16 ms dephasing time. The dephasing of the high-field line at 15 ppm allows the unique assignment of this line to the $^{13}C^{\beta}$ of residue Ala55.

SH3 domain sample (not shown) exhibits a strong line overlap in the central region of the spectrum. In the low-field range, lines are visible which can be attributed to the tryptophan ring ^{15}N of Trp41 and Trp42 by comparison with the liquid-state ^{15}N NMR spectrum.

In the next step, the $^{13}C-^{15}N$ REDOR decay curves of the selectively labeled sample were recorded employing XY-16 phase cycling at 5 kHz rotation frequency. Because of the better chemical shift dispersion in the ^{13}C MAS regime, a version of the REDOR experiment with observation of ^{13}C was chosen, where all π pulses except the central echo pulse are irradiated in the ^{15}N channel. A strong REDOR effect on the $^{13}C^{\beta}$ of Ala55 residue is visible. The resulting REDOR data are shown in Fig. 7. For the simulation of the REDOR data, the ^{15}N labeling factor of the tryptophan N^{ring} had to be taken into account by multiplying the REDOR curve [Eqn (7)] with the mole fraction of the ^{15}N-labeled tryptophan. From the simulation of the REDOR curve, using Eqn (7), a dipolar coupling of $D = 48 \pm 8$ Hz is determined. This dipolar coupling can be converted into a $^{13}C-^{15}N$ distance of 4.02 ± 0.23 Å. It was shown by Garbow *et al.*[51] that fast molecular vibrations cause a modulation of the CN distance which, owing to the partial averaging of the dipolar interaction, leads to a decrease in the dipolar coupling and thus to an elongation of the determined distance. Such effects lead to a typically 10% reduction of the dipolar coupling measured by REDOR. Correcting the dipolar coupling with this reduction factor of 10%, a motionally corrected dipolar coupling of 53 ± 8 Hz is found, corresponding to a CN distance of 3.85 ± 0.25 Å.

There are small differences in the CN distance obtained by other spectroscopic techniques: on the one hand, the (Ala55, C^{β}) (Trp42, N^{ring}) distances obtained by several x-ray diffraction studies[40,41,43] vary in the range 3.56–3.66 Å; on the other hand, by liquid-state NMR spectroscopy[42] an (Ala55, C^{β}) (Trp42, N^{ring}) distance of 3.73 Å is found. This variation in the (Ala55, C^{β}) (Trp42, N^{ring}) distance is already an indication of some structural

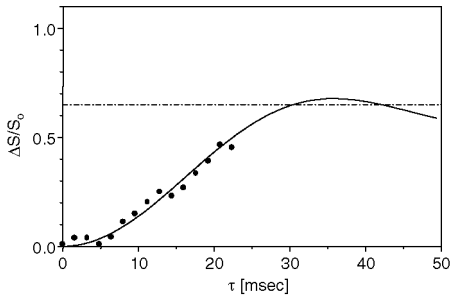

Figure 7. ^{13}C ^{15}N REDOR data of $^{13}C^{\beta}$ (Ala55) of the selectively labeled SH3 domain sample. Owing to T_2 relaxation, only data with $\tau < 20$ ms are used for the evaluation of the coupling. The dashed line at $\Delta S/S_0 = 0.65$ marks the final value expected from the ^{15}N isotope labeling factor of the tryptophan. The solid line is calculated from Eqn (7), employing a weighted superposition of 65% alanine-$^{13}CH_3$ tryptophan-^{15}N and 35% alanine-$^{13}CH_3$ tryptophan-^{14}N, resulting in a dipolar coupling of $D = 48 \pm 8$ Hz, which after correction for fast molecular vibrations yields a CN distance of 3.85 ± 0.25 Å.

freedom of the tryptophan side-chain. Comparing these values with the REDOR value of 3.85 ± 0.25 Å, it is evident that the motionally corrected REDOR distance, in the limits of the error margins, agrees with the x-ray distance. However, the REDOR distance is slightly (0.1–0.2 Å) longer than the average x-ray distance. In the following we analyze whether (i) this difference between the x-ray and REDOR distances is simply the result of experimental errors or whether (ii) a structural change of the SH3 domain can reasonably account for this difference.

(i) The dipolar coupling extracted from the REDOR data depends on the knowledge of the final value of the REDOR curve, which is determined by the isotope labeling factor of the ^{15}N nucleus. Owing to the restricted sensitivity of the 7 T spectrometer, the short T_2 relaxation time of the alanine-$^{13}C^{\beta}$ signal and the small available amount of sample, it was not possible to follow the REDOR decay further than about 20 ms and the complete REDOR dephasing of the REDOR signal could not be observed. Therefore, we had to calculate the final value of the REDOR curve from the experimentally determined ^{15}N labeling factor, which has an uncertainty of ca ±5%. A calculation with a ^{15}N labeling factor of 60% instead of 65% results in a motionally corrected $^{13}C-^{15}N$ dipolar coupling of 59 ± 8 Hz, corresponding to a CN distance of 3.75 ± 0.20 Å, which is in very good agreement with the CN distances obtained from liquid-state NMR spectroscopy. As will be shown below, this dependence of the REDOR evaluation on the isotope labeling can be avoided by the application of a combined TEDOR–REDOR experiment.

(ii) The structure of the SH3 domain studied in this work is different from the structures studied by x-ray and liquid-state NMR spectroscopy, owing to the sample preparation. The spread of the distances observed by the other techniques already suggests that there is some structural freedom of the SH3 molecule concerning this distance. In particular, the x-ray structure suggest that the trytophan side-chain (see Fig. 1) has a relatively large free volume for reorientations at its disposal, since the closest distances of the van der Waals spheres of the atoms of the tryptophan side-chain and the neighboring side-chains are between ca 0.5 and 1 Å. Therefore, it may be possible that the moistening of the sample, which was necessary to achieve the best resolution in the NMR spectra, causes a partial different structure of this region of the molecule. In particular, a change of the molecular conformation, either in the form of a rotation of the

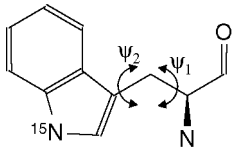

Figure 8. Sketch of the tryptophan residue. The distance between the ring nitrogen and the alanine-$^{13}C^{\beta}$ depends on the torsional angles ψ_1 and ψ_2.

tryptophan ring or in the form of a slight rearrangement of the backbone chain, could have occurred, e.g. owing to water molecules which have diffused into the 'free' volume close to the tryptophan ring. To achieve a quantitative estimation of the structural changes, necessary for obtaining the found difference in the distance data, we studied the influence of the orientation of the tryptophan side-chain on the distance. Figure 8 defines the torsional angles ψ_1 and ψ_2. Calculations with a molecular modeling program show that ψ_2 has only a minor influence on the CN distance, but that the distance depends very strongly on ψ_1. In particular, a change of 4° in ψ_1 leads to a change of 0.3 Å in the CN distance, which corresponds to the difference between the REDOR distance of 3.85 Å and the shortest x-ray distance of 3.56 Å. Hence the assumption that torsional rotations of the tryptophan side-chain, caused for example by the moistening of the sample, are responsible for the variations in the x-ray data, and also the difference between x-ray and REDOR distance, is compatible with the structure of the protein in the vicinity of the tryptophan.

From the present data it is not possible to distinguish between these two alternatives, namely a systematic error in the REDOR curve, which is introduced by the isotope labeling factor, and a structural change of the molecule, and it is therefore not possible to draw a final conclusion about a structural change induced by the moistening of the sample.

It should be noted that the problem of accurately determining the labeling factor can be avoided by a combination of spectral and chemical editing. A possible example of such an experiment is a $^{15}N-^{13}C$ TEDOR transfer followed by the $^{13}C-^{15}N$ REDOR sequence. After the initial TEDOR sequence only those ^{13}C spins that are polarized by ^{15}N neighbors show a signal. This corresponds to an effective labeling factor of 100%. The problem with this approach is the loss in sensitivity in the TEDOR step, because only a partial coherence transfer from ^{15}N to ^{13}C is possible. To overcome this loss in sensitivity it is necessary to work at higher fields. Hence, for example, on a 14 T solid-state NMR spectrometer such combined TEDOR–REDOR experiments should be feasible.

CONCLUSION

Whereas in previous work we studied only small molecules with REDOR spectroscopy, in this work a real protein, namely the SH3 domain of α-spectrin (chicken), was studied as a model compound for the application of $^{15}N-^{13}C$ TEDOR and $^{13}C-^{15}N$ REDOR NMR spectroscopy. For these experiments, two different SH3 samples were synthesized and measured, namely a nominally 100% ^{13}C- and ^{15}N-labeled, lyophilized sample for the TEDOR experiment, and a selectively alanine $^{13}C^{\beta}$- and tryptophan $^{15}N^{ring}$-labeled sample, precipitated from solution, for the REDOR experiment. In a first step it was shown that the TEDOR experiment can be employed as a very efficient dipolar filter for spectral editing of the ^{13}C MAS spectrum. In a second step, the TEDOR sequence was employed as the contact sequence in the evolution period of a 2D solid-state heteronuclear correlation (HETCOR) experiment, allowing us to distinguish between those ^{13}C coupled to backbone ^{15}N and those ^{13}C coupled to lysine side-chain $^{15}N^{\varepsilon}$. Finally, the inter-residual distance between the alanine-C^{β} (Ala55) and the tryptophan (Trp42) $^{15}N^{ring}$ was measured by $^{13}C-^{15}N$ REDOR spectroscopy. The REDOR measurements immediately allow one to attribute uniquely the dephasing ^{13}C line to the Ala55 residue. From the REDOR data the dipolar $^{15}N-^{13}C$ coupling is determined, and after correction for fast molecular vibrations and motions, converted into a CN distance of 3.85 ± 0.25 Å, which is very close to but slightly larger than the CN distances found by x-ray diffraction and liquid-state NMR (3.56–3.66 and 3.73 Å, respectively). This enlargement of the distance might be an indication of a conformational change of the SH3 domain e.g. due to the sample preparation, but it cannot be excluded that it is the result of the errors in the experimental determination of the ^{15}N labeling factor. As a possible solution of this question a combined application of TEDOR and REDOR is discussed, which, however, is feasible only on a solid-state NMR spectrometer with higher field, i.e. higher sensitivity.

Acknowledgments

We thank Martina Leidert of the FMP for the preparation of the SH3 domain samples. This work was financially supported by the German Israel Foundation, grant GIF I-595-43.09/98. J. P. is supported by the Hochschulsonderprogramm (HSP) III.

REFERENCES

1. Garrett RH, Grisham CM. *Biochemistry*. Saunders: Philadelphia, 1995.
2. Ernst R, Bodenhausen G, Wokaun A. *Principles of NMR in One and Two Dimensions*. Clarendon Press: Oxford, 1987.
3. Evans JNS. *Biomolecular NMR Spectroscopy*. Oxford University Press: Oxford, 1995.
4. Slichter CP. *Principles of Magnetic Resonance*. (3rd edn). Springer: Berlin, 1990.
5. Schmidt-Rohr K, Spiess HW. *Multidimensional Solid State NMR and Polymers*. Academic Press: London, 1994.
6. Bechinger B, Opella SJ. *J. Magn. Reson.* 1991; **95**: 585.
7. McDonnel P, Shon K, Kim Y, Opella SJ. *J. Mol. Biol.* 1993; **233**: 447.
8. Andrew ER, Bradbury A, Eades RG. *Nature* 1958; **182**: 1659.
9. Lowe IJ. *Phys. Rev. Lett.* 1959; **2**: 285.
10. Schaefer J, Stejskal EO, Buchdahl R. *Macromolecules* 1975; **8**: 291.
11. Schaefer J, Stejskal EO. *J. Am. Chem. Soc.* 1976; **98**: 1031.
12. Bennett AE, Griffin RG, Vega S. *Springer Ser. NMR* 1994; **33**: 1.
13. Auger M. *J. Chim. Phys. Phys. Chim. Biol.* 1995; **92**: 1751.
14. Gullion T, Schaefer J. *Adv. Magn. Opt. Res.* 1989; **13**: 57.
15. Gullion T, Schaefer J. *J. Magn. Reson.* 1989; **81**: 196.
16. Schimming V, Hoelger CG, Buntkowsky G, Sack I, Fuhrhop JH, Rocchetti S, Limbach H-H. *J. Am. Chem. Soc.* 1999; **121**: 4892.
17. Sack I, Macholl S, Fuhrhop JH, Buntkowsky G. *Phys. Chem. Chem. Phys.* 2000; **2**: 1781.
18. Sack I, Goldbourt A, Vega S, Buntkowsky G. *J. Magn. Reson.* 1999; **138**: 54.
19. Holl SM, Marshall GR, Beusen DD, Kociolek K, Redlinski AS, Le-Plawy MT, McKay RA, Vega S, Schaefer J. *J. Am. Chem. Soc.* 1992; **114**: 4830.
20. McDowell LM, Schmidt A, Cohen ER, Studelska DR, Schaefer J. *J. Mol. Biol.* 1996; **256**: 160.

21. McDowell LM, Klug CA, Beusen DD, Schaefer J. *Biochemistry* 1996; **35**: 5395.
22. McDowell L, Lee M, McKay RA, Anderson KS, Schaefer J. *Biochemistry* 1996; **35**: 3328.
23. Li Y, Krekel F, Ramilo CA, Amrhein N, Evans JNS. *FEBS Lett.* 1995; **337**: 208.
24. Heller J, Kolbert AC, Larsen R, Ernst M, Bekker T, Baldwin M, Prusiner SB, Pines A, Wemmer DE. *Protein Sci.* 1996; **5**: 1655.
25. Klug CA, Studelska DR, Chen G, Gilbertson SR, Schaefer J. *Solid State Nucl. Magn. Reson.* 1996; **7**: 173.
26. Weliky DP, Tycko R. *J. Am. Chem. Soc.* 1996; **118**: 8487.
27. Wang J, Balasz YS, Thompson LK. *Biochemistry* 1997; **36**: 1699.
28. Goetz JM, Poliks B, Studelska DR, Fischer M, Kugelbrey K, Bacher A, Cushman M, Schaefer J. *J. Am. Chem. Soc.* 1999; **121**: 7500.
29. Sack I, Macholl S, Wehrmann F, Albrecht J, Limbach HH, Fillaux F, Baron MH, Buntkowsky G. *Appl. Magn. Reson.* 1999; **17**: 413.
30. McDowell LM, Holl SM, Qian S, Li E, Schaefer J. *Biochemistry* 1993; **32**: 4560.
31. Christensen AM, Schaefer J. *Biochemistry* 1993; **32**: 2868.
32. Griffith JM, Griffin RG. *Anal. Chim. Acta* 1993; **283**: 1081.
33. Beusen DD, McDowell LM, Slomczynska, Schaefer J. *J. Med. Chem.* 1995; **38**: 2742.
34. Fyfe CA, Mueller KT, Grondey H, Wongmoon KC. *Chem. Phys. Lett.* 1992; **199**: 198–204.
35. Fyfe CA, Mueller KT, Grondey H, Wongmoon KC. *J. Phys. Chem.* 1993; **97**: 13484–13495.
36. Fyfe CA, Wongmoon KC, Huang Y, Grondey H, Mueller KT. *J. Phys. Chem.* 1995; **99**: 8707.
37. Fyfe CA, Wongmoon KC, Huang Y, Grondey H. *Microporous Mater.* 1995; **5**: 29.
38. Fyfe CA, Wongmoon KC, Huang Y, Grondey H. *J. Am. Chem. Soc.* 1995; **117**: 10397.
39. Hing A, Vega S, Schaefer J. *J. Magn. Reson.* 1992; **96**: 205.
40. Musacchio A, Noble M, Pauptit R, Wierenga R, Saraste M. *Nature (London)* 1992; **359**: 851.
41. Morton CJ, Pugh DJR, Brown ELJ, Kahman JD, Renzoni DAC, Campbell ID. *Structure* 1996; **4**: 705.
42. Blanco FJ, Oritz AR, Serrano L. *J. Biomol. NMR* 1997; **9**: 347.
43. Musacchio A, Gibson T, Veli-Pekka L, Saraste M. *FEBS Lett.* 1992; **307**: 55.
44. Mueller KT, Jarvie TP, Aurentz DJ, Roberts BW. *Chem. Phys. Lett.* 1995; **242**: 535.
45. d'Espinose de la Caillerie J, Fretigny C. *J. Magn. Reson.* 1998; **133**: 273.
46. Studelska DR, Klug CA, Beusen DD, McDowell LM, Schaefer J. *J. Am. Chem. Soc.* 1996; **118**: 620.
47. Horii F, Hirai A, Kitamaru R, Sakurada I. *Cell. Chem. Technol.* 1985; **19**: 513.
48. Buntkowsky G, Sack I, Limbach H-H, Kling B, Fuhrhop J. *J. Phys. Chem. B* 1997; **101**: 11265.
49. Bennett AE, Rienstra CM, Auger M, Lakshmi KV, Griffin RG. *J. Chem. Phys.* 1995; **103**: 6951.
51. Mitchell D, Evans J. *Mol. Phys.* 1998; **95**: 907.
51. Garbow J, Gullion T. *Carbon-13 NMR Spectroscopy of Biological Solids*. Academic Press: New York, 1995.
52. Pauli J, Van Rossum B, Förster H, de Groot HJM, Oschkinat H. *J. Magn. Reson.* 2000; **143**: 411.

